Correlation between *in Vitro* Peptide Binding Profiles and Cellular Activities for Estrogen Receptor-Modulating Compounds

MARIE A. IANNONE, CATHERINE A. SIMMONS, SUE H. KADWELL, DANIEL L. SVOBODA,
DANA E. VANDERWALL, SU-JUN DENG, THOMAS G. CONSLER, JEAN SHEARIN, JOHN G. GRAY,
AND KENNETH H. PEARCE

Department of Gene Expression and Protein Biochemistry (M.A.I., C.A.S., S.H.K., S.-J.D., T.G.C., J.S., J.G.G., K.H.P) and Department of Cheminformatics (D.L.S., D.E.V.), Discovery Research, GlaxoSmithKline, Research Triangle Park, North Carolina 27709

Numerous biochemical and structural studies have shown that the conformation of the estrogen receptor α (ERα) can be influenced by ligand binding. In turn, the conformational state of ERα affects the ability of the receptor to interact with a wide variety of protein accessory factors. To globally investigate ligand-based cofactor recruitment activities of ERα, we have applied a flow cytometric multiplexed binding assay to determine the simultaneous binding of ERα to over 50 different peptides derived from both known cofactor proteins and random peptide phage display. Using over 400 ERα-binding compounds, we have observed that the multiplexed *in vitro* peptide-binding profiles are distinct for a number of compounds and that these profiles can predict the effect that ERα ligands have on various cellular activities. These cell-based activities include transcriptional regulation at an estrogen response element, MCF-7 cell proliferation, and Ishikawa endometrial cell stimulation. The majority of the compound-induced diversity in the peptide profiling assay is provided by the unique phage display peptides. Importantly, some of these peptides show a sequence relationship with the corepressor motif, suggesting that peptides identified via phage display might represent natural binding partners of ERα. These *in vitro*: cellular correlations may in part explain tissue-specific activities of ERα-modulating compounds. (*Molecular Endocrinology* 18: 1064–1081, 2004)

THE ESTROGEN RECEPTOR (ER) is a multifunctional, pharmaceutically relevant transcription factor that serves to transduce the activities of estrogens through both protein-protein and protein-DNA interactions. A wide variety of protein binding partners for ER have been discovered and characterized, including nuclear coregulator accessory proteins (1, 2), cytoplasmic kinases (3, 4), and transcription factors (5, 6). It is clear that ER plays an important role in a number of interrelated signal transduction pathways.

Abbreviations: aa, Amino acids; AF1, activation function 1; AF2, activation function 2; AIB1, amplified in breast cancer 1; AP-1, activator protein-1; cpm, radioactive counts per minute; DAX, dosage-sensitive sex reversal-adrenal hypoplasia congenita critical region on the X chromosome; DES, diethylstibestrol; ERα, estrogen receptor α; ERE, estrogen response element; LBD, ligand-binding domain; MFI, mean fluorescent intensity; NCoR, nuclear receptor corepressor; NF-κB, nuclear factor-κB; PCA, principal components analysis; PGC-1α, peroxisome proliferator-activated receptor γ coactivator-1 α; RIP140, receptor-interacting protein 140; SERMS, selective ER modulators; SHP, short heterodimer partner; SMRT, silencing mediator of retinoic acid and thyroid receptor; SRC-1, steroid receptor coactivator-1; STAT5, signal transducer and activator of transcription 5; TIF2, transcriptional intermediary factor 2.

Molecular Endocrinology is published monthly by The Endocrine Society (http://www.endo-society.org), the foremost professional society serving the endocrine community.

Two different ER genes have been identified, yielding the two sequence-related protein products, ERα and ERβ (7, 8). Although ERβ is an important participant in the estrogen response, several studies suggest that ERα is responsible for much of the physiology associated with estrogens and estrogen replacement therapy (9, 10). It is commonly accepted that estrogens bind to the ligand-binding domain (LBD) of ERα and elicit, among many other activities, an increase in transcriptional activity for genes containing some form of an estrogen response element (ERE) within the promoter region. This transactivation activity is enhanced by the ligand-induced association of cofactor or coactivator proteins, such as steroid receptor coactivator-1 (SRC-1) or cAMP response element binding protein-binding protein (CBP) (11).

Numerous crystal structures have confirmed that the most C-terminal α helix, typically helix 12 known as the activation function or AF helix, of the receptor is prone to conformational flexibility (12–14). Agonist ligands such as estradiol and diethylstilbestrol (DES), tend to stabilize the AF helix into a position that exposes a hydrophobic patch or groove that can accept an amphipathic helix presented by cofactor proteins. These short helical regions, called NR boxes, usually occur in multiples within the cofactor protein and typically contain an LXXLL motif (where L is leucine and X is any amino acid) (15). Antagonist ligands, such as

EXHIBIT T

tamoxifen and raloxifene, force helix 12 into a position where it occupies the coactivator binding site and consequently blocks the intermolecular association of the coactivator amphipathic helix (12).

The conformational flexibility of helix 12 is an important feature of nuclear receptors and can allow for the design of ER-modulating ligands that shift the dynamic equilibrium between multiple states. In addition, nuclear magnetic resonance studies with another structurally related nuclear receptor have shown that ligands can affect the conformational dynamics in other regions of the LBD in addition to the AF helix (16). The conclusion of these structural studies was that subtle modifications of the ligand produce significant effects on the conformation of the LBD in multiple regions. In light of the emerging structural and functional work on ERα and its LBD, there is an ongoing quest to find new selective ER modulators (SERMs) that may induce unique conformations. In addition to the well-known molecules raloxifene and tamoxifen, a new class of modulators might retain more of the beneficial effects of estrogen without the undesired side effects (17).

Similar to the conformational complexity of the LBD, ERα performs a myriad of signal transduction functions once bound with ligand. The complexity of ERα signaling is demonstrated by the observation that genes can be regulated either directly, through binding to EREs, or indirectly, through influencing the function of other proteins such as nuclear factor-κB (NF-κB), activator protein-1 (AP-1), MAPK, or STAT5 (6, 18–21). Concerning the well-studied ability of ERα to repress NF-κB-driven gene expression, the precise molecular mechanism for this activity remains unresolved and controversial (20). Several models have been proposed and one of these includes the direct physical interaction of ER with either the p50 or p65 subunit of NF-κB (22, 23). In addition to interaction with transcription factors, it has been shown that activated ERα can alter pathways in the cytoplasm, such as kinase phosphorylation cascades. These effects of ER are generally referred to as nongenomic activities. It is becoming more apparent that these functions are a significant part of the ERα activity repertoire (24). The development of the next generation of SERMs will need to consider numerous ER activities.

To rapidly characterize the various protein-binding functions of ligand-activated ERα as represented by peptide surrogates, we have used a method that can essentially reconstruct a simplified *in vitro* cellular environment for the receptor. This multiplexed technique allows simultaneous monitoring of up to 100 ligand-modulated interactions. Through the use of fluorescently distinct microsphere populations, individual peptides, for example peptides representing LXXLL NR boxes from coactivators or sequences identified via phage display, can be coupled to separate microsphere populations. Flow cytometric analysis of the microspheres simultaneously decodes each population and also detects receptor binding to respective peptides. Use of this fluorescent microsphere multiplexed binding assay has been previously demonstrated for nuclear receptor interactions (25), as well as several other applications (26, 27).

This binding-partner profile represents, in part, opportunities that the ER has to interact with partners in a cellular environment. In addition, phage display identified peptide sequences have the potential to represent currently unrecognized cellular interaction partners. These peptide interactions represent the starting signal for cellular outcomes driven through the ERα, such as gene regulation, cytokine production, cell proliferation, and cell stimulation. To acquire more evidence that peptide binding profiles reflect ERα biology, we have used a large number (>400) of ER-binding compounds that have varying degrees and directions of modulating activities and we have obtained both binding profiles and cell-based activities for these compounds. We have found that a number of peptide binding profiles correlate well with cellular activities. For this report, we have used several cell-based assays to explore the ability of ligand-activated ERα to effect 1) transcription of a reporter gene via an ERE, 2) the proliferation of a breast cancer cell line, and 3) the stimulation of an endometrial-derived cell line.

As described in this paper, a simplified *in vitro* binding assay for monitoring the myriad of activities of the ERα can be a great aid in helping to predict and understand the cellular outcomes of modulating ligands. Using the compounds as the link between these two types of assays, *in vitro* and *cellular*, we have been able to make distinct correlations between peptide binding events and cell-based assay activities imparted by novel ERα ligands.

RESULTS

Peptide Tools for Compound Profiling

Previous work has demonstrated that recombinant peptide libraries, such as phage display, are a powerful way of identifying peptides that selectively bind to nuclear receptors (28–30). Our initial efforts to identify selective conformation-sensing peptides used a random 10-residue peptide library displayed as a fusion to the gene III coat protein of filamentous bacteriophage (31). Several of the conformation-sensing peptides selected against ERα are shown in Table 1. Typically, with selection *vs.* ERα LBD bound to an agonist ligand such as estradiol or DES, we readily identified LXXLL-containing peptides after a single round of sorting. However, not all peptides that bound to the ERα LBD-estradiol complex contained the NR box motif. One example is the peptide denoted K7P2 as shown in Table 1. K7P2 binds to ERα LBD in the presence of many different estradiol-like ligands with the same behavior as a classical LXXLL, but does not contain a typical leucine motif. In contrast, clones

EXHIBIT T

selected *vs.* antagonist-bound ERα LBD, such as raloxifene, tamoxifen, idoxifene, and levermeloxifene, yielded only non-LXXLL peptide sequences. Several novel ERα LBD compound-selective peptides were identified including I8P2 for idoxifene, R5P2 for raloxifene, and GW5P2 for GW5638 or its 4-hydroxyl metabolite, GW7604. Although we were able to successfully isolate peptides with the random 10-residue peptide library, it is evident from sibling DNA sequences of selected peptides that the size of the original library limits peptide diversity.

To isolate peptides of higher affinity and greater specificity to the ERα LBD-GW7604 complex, we made a second-generation phage display library on a phagemid vector for soft randomization or affinity maturation (32–34). This library was based on the sequence of the GW5P2 clone. Each of the ten residues was randomized with a bias toward the original codon using 80% of the bases from the original template sequence and an equal mixture of the three other bases at 20%. Three additional randomized codons were added to both ends of the original sequence. By sorting this library against ERα LBD in the presence of GW7604 (or other compounds with an acrylate head group), we identified peptide sequences 47P3 and 33P4. Although this peptide library was re-randomized, the selected acrylate-sensing peptide sequences retained the original LF(E/D)RVWLRE(L/H) motif of GW5P2 (Table 1). An additional leucine residue was selected in the three randomized codon regions at both the N and C terminus. These extra hydrophobic residues may account for the increased affinity of 47P3 for ERα compared with the original GW5P2 peptide (demonstrated by increased binding signal; see Fig. 2B).

In addition to 10 peptides identified with phage display, 48 synthetic peptides containing the binding motifs from 18 coactivator proteins, two coregulator proteins [*i.e.* DAX (dosage-sensitive sex reversal-adrenal hypoplasia congenita critical region on the X chromosome) and SHP (short heterodimer partner)] and two corepressor proteins (Table 1 and Ref. 25) were used. These peptides were typically about 25 amino acids in length with a biotin at the amino terminus.

Multiplexed-Peptide Binding Assay

To efficiently assess the effects of 405 ERα-binding compounds on ERα binding to 58 peptides representing the binding motifs of coactivator, coregulator, and corepressor proteins as well as compound-selective phage display peptide sequences, we employed a modified microsphere-based binding assay that has been described previously (25). All compounds within
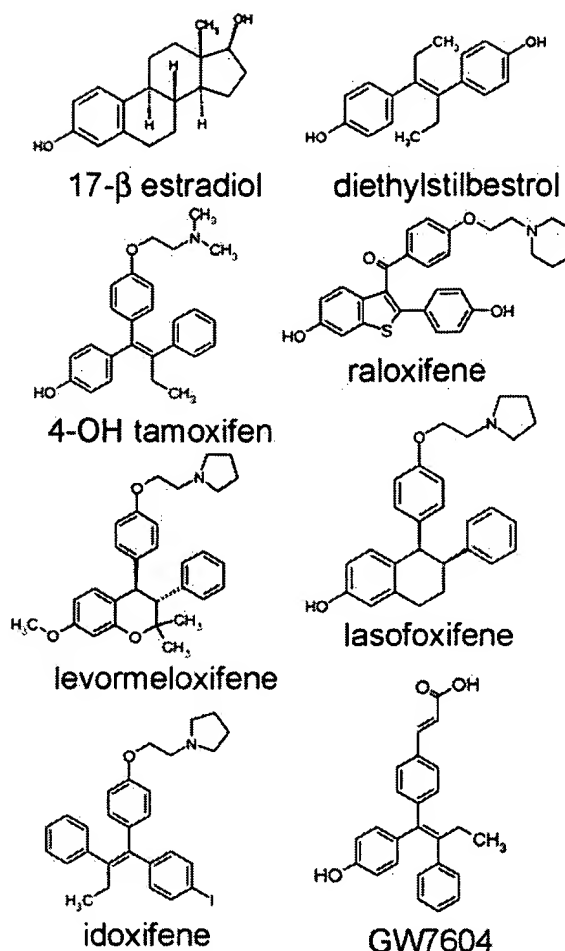

Fig. 1. Structures of ERα Tool SERM Compounds

this set were determined to bind ERα with a $pK_i \geq 6.0$. We included several classic, well-characterized ERα ligands such as estradiol, DES, raloxifene, 4-OH tamoxifen, idoxifene, levormeloxifene, lasofoxifene, and GW7604 (35) (Fig. 1) within the 405 compound set. Binding of Alexa532-labeled ERα LBD is reported in mean fluorescence intensity units (MFI). Under the conditions of the assay, the MFI is proportional to affinity of peptide binding (25).

In the absence of compound, ERα LBD binds to many of the peptides (Fig. 2A). Compounds may modulate the interaction of ERα with peptide by enhancing or inhibiting this basal interaction. Typically, to demonstrate the effect of compound on ERα peptide-recruitment activity, we subtract the basal value from the value obtained in the presence of compound. Therefore, if a compound enhances a binding interaction, the data point will have a value greater than zero and alternatively, if the interaction is inhibited it will

Fig. 2. Peptide Profile Plots for ERα

Alexa 532-labeled ERα LBD (10 nM) was incubated with 58 fluorescently unique, peptide-coupled microsphere populations for 1.5 h in the presence or absence of compound (1 μM). The fluorescence associated with each microsphere was determined by flow cytometry. A, Binding of ERα LBD to peptides in the absence of compound. B, Binding of ERα LBD to peptides in the

EXHIBIT T

A

B

C
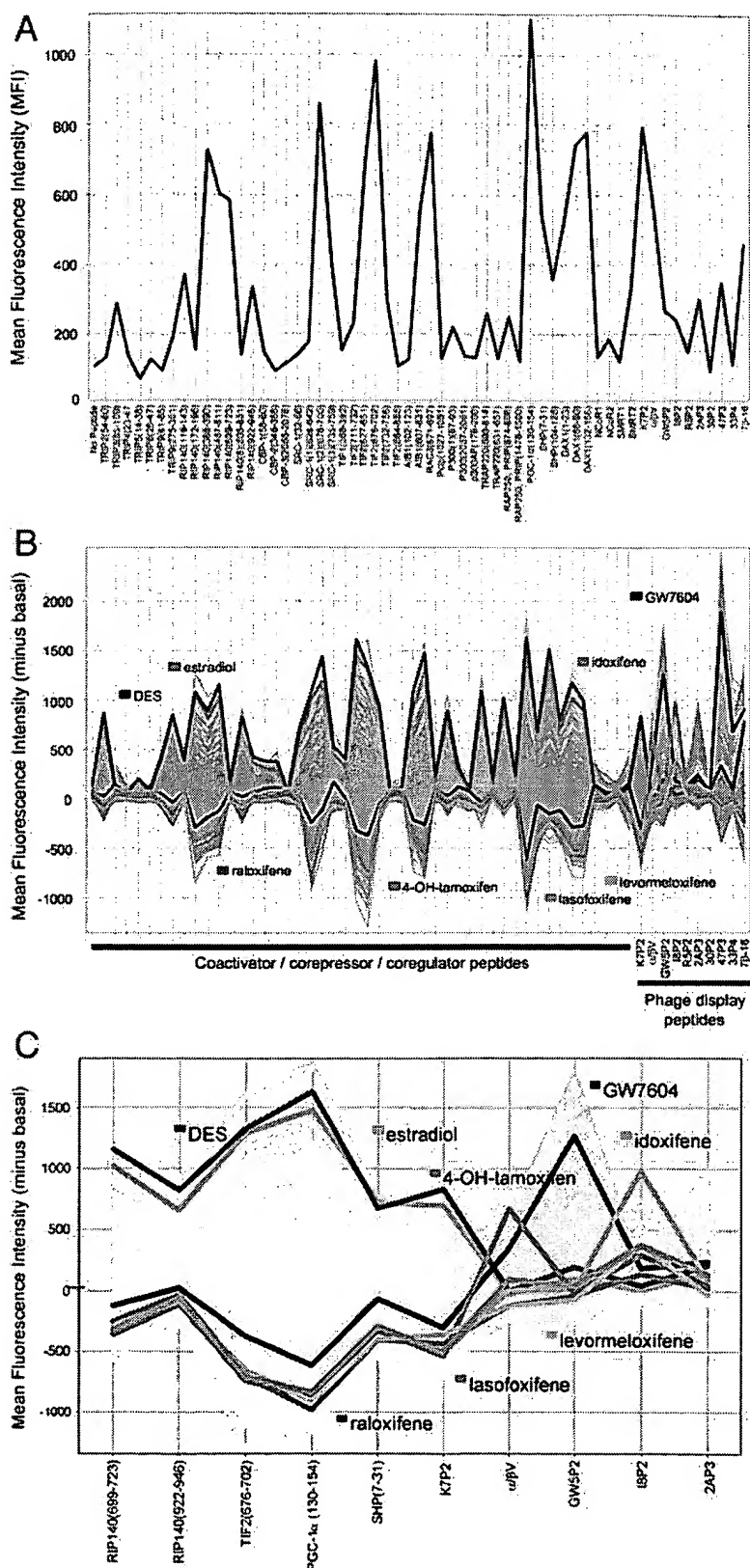
presence of compound. Each *line* represents the binding profile for one of 405 compounds where basal binding (no compound) has been subtracted. Binding profiles for tool SERM compounds are color-coded. Other compounds tested are shown as *gray* in the background. C, ERα LBD binding in the presence of tool SERM compounds (color scheme as above) for peptides selected by principle component analysis (basal binding has been subtracted). Most data points represent the mean from 10 separate binding experiments.

EXHIBIT T

have a value less than zero. Figure 2B highlights the binding profiles of ERα LBD for 58 peptides in the presence of estradiol, DES, 4-OH tamoxifen, raloxifene, GW7604, idoxifene, lasofoxifene, and levormeloxifene. Each line represents binding data for one compound across the set of peptides. Other compounds examined are shown as *gray lines* in the background. Estradiol and DES enhanced the binding of ERα LBD to coactivator and coregulator peptides as well as to the pan-agonist phage-identified peptide K7P2. In contrast, 4-OH tamoxifen, raloxifene, GW7604, idoxifene, and levormeloxifene all inhibited ERα LBD basal binding to coactivator and coregulator peptides. 4-OH tamoxifen enhanced the binding of ERα LBD to the tamoxifen-selective peptide sequence α/βV (29), and GW7604 promoted ERα LBD binding to the peptides GW5P2, 47P3, and 33P4. Idoxifene, and to some degree levormeloxifene and lasofoxifene, enhanced ERα LBD binding to I8P2.

Shape-Based Clustering of Peptide Binding Profiles

Many of the peptides fall into groups that either behave similarly in the presence of compound or do not bind ERα LBD. To identify these peptide sets and reduce possible statistical bias, principal components analysis (PCA) was conducted using binding data from the 405 compound set. PCA reduced the number of peptides in the set from 58 to 10 representative peptides that account for approximately 99% of the variation in the data (see *Data Reduction Methods*). Figure 2C shows the same binding data from Fig. 2B after peptide selection by PCA. Interestingly, we have found that most of the coactivator binding trends for these compounds on ERα LBD could be described by data from receptor-interacting protein 140 (RIP140) (699–723), RIP140 (922–946), transcriptional intermediary factor 2 (TIF2) (676–702), peroxisome proliferator-activated protein γ coactivator-1 α (PGC-1α) (130–154), and SHP (7–31). From the data shown in Fig. 2, B and C, it is evident that most of the compounds affect coactivator peptides in the same manner. In other words, if a compound promotes ERα LBD binding to one LXXLL peptide it will most likely do so for other LXXLL peptides (especially for peptides that bound in the absence of compound). Subsequent clustering of the profile data was conducted, using the 10 peptide variables, as shown in Figs. 3 and 4.

Using a cutoff of 12 clusters, depicted by the dendrogram in Fig. 3, Fig. 4 shows the shape-based clustering results from the 405 binding profiles. A number of compounds yielded profiles that were relatively muted in terms of peptide recruitment. These compounds fall into cluster 1 (178 compounds) and cluster 2 (45 compounds). Clusters 3 (three compounds), 4 (14 compounds), and 5 (32 compounds) can be described as agonist or estradiol like. Compounds in these clusters show significant coactivator and K7P2 peptide recruitment with little effect on ERα LBD bind-

ing to corepressor and most phage-derived peptides. Clusters 6 (two compounds), 7 (33 compounds), and 8 (59 compounds) are each unique and contain the tool compounds idoxifene, 4-OH tamoxifen, and raloxifene/lasofoxifene/levormeloxifene, respectively. Although ERα LBD binding to coactivator peptides is inhibited for all the compounds that fall within clusters 6–8, the unique binding attribute of each of these clusters comes from the phage display peptides. Cluster 9 (1 compound) shows a profile somewhat similar to that for the 4-OH tamoxifen cluster 7. The final three clusters, cluster 10 (27 compounds), 11 (one compound), and 12 (10 compounds), contain variations of profiles that show binding to the GW5P2 peptide. In addition, many compounds in cluster 12 (and some found in cluster 10) also yield significant recruitment of 2AP3, which is a phage peptide identified with a GW7604-like ligand. Overall, this analysis shows that different ERα ligands have the ability to differentially effect peptide recruitment and that these differences can be used to group compounds using a hierarchical clustering routine.

Correlation of Cellular Function with Peptide Binding Profile

Several cell-based assays were used to further characterize a subset of the 405 ERα compounds. A transient transfection assay was used to assess the ability of compounds to drive reporter gene expression via the consensus vitellogenin ERE promoter (36). Compounds were evaluated for their ability to stimulate transcriptional activity (agonist mode, Fig. 5A). Those that did not show agonist activity were evaluated for their ability to antagonize or inhibit transcriptional activity of a subsaturating dose of estradiol (antagonist mode, Fig. 5B). To incorporate the pEC_{50} and pIC_{50} with efficacy values from the full dose-response curve fits, the potency measurement reported on the x-axis is the product of the two (where efficacy is a percentage relative to either estradiol or raloxifene standards). In cases where we have full dose-response curves, we chose to display the data in this manner because it incorporates both measured parameters. Trends are the same using only efficacy values, but the correlation with peptide binding data is improved when accounting for EC_{50} or IC_{50} value. As shown in Fig. 5A, a subset of ligands was examined for their effects on binding to the SRC-1(2) peptide (*blue squares*) and also for agonist activity at an ERE. These same ligands were also tested for binding to peptides from amplified in breast cancer 1 (AIB1) (607–631) (*green triangles*), K7P2 phage derived (*red circles*), PGC-1α (130–154) (*yellow triangles*), DAX1 (132–156) (*cyan hexagons*), and TIF2 (676–702) (*red triangles*). There is a general trend of increased ERE potency relative to coactivator peptide recruitment. Similarly, those compounds most effective at antagonizing the activity of estradiol show the most negative peptide recruitment values (Fig. 5B).
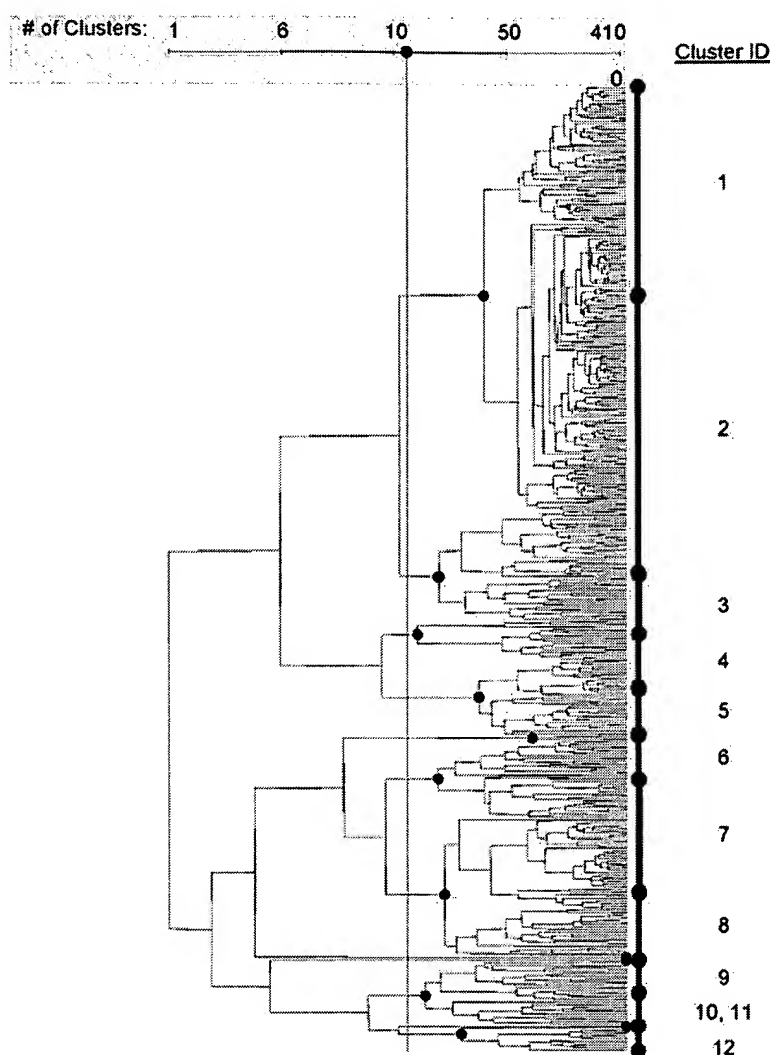
EXHIBIT T

Fig. 3. Dendrogram Showing Relationship of Peptide Binding Profiles
      Peptide binding profiles were analyzed using both principle component analysis and a hierarchical clustering routine using a similarity measure based on a profile's shape. The resulting dendrogram shows the relationship between clusters and the vertical line (at 12) indicates the level chosen for display of clusters.

A subset of the 405 compounds was also tested for the ability to induce cell proliferation of MCF-7 breast cancer cells as determined by [^{3}H]thymidine incorporation (37, 38). A full dose-response curve was performed for these compounds and efficacies were normalized to an estradiol standard. Typically, estradiol yielded about an 8-fold increase in [^{3}H]thymidine incorporation compared with the no compound control. Some compounds decreased the basal level of proliferation. For these compounds, the fit of the negative dose response yielded an IC_{50} value and a minimum signal. This minimum signal was normalized to that obtained for raloxifene. The x-axis of Fig. 6 shows the potency of the compounds expressed as the product pEC_{50} or pIC_{50} (where pIC_{50} are negative values) and the normalized efficacy value; the y-axis shows peptide data for these same compounds where *blue squares* represent binding data for SRC-1(2) (676–700)

peptide and other *colored symbols* represent five additional peptides. As shown, there is a general trend toward increased coactivator recruitment and increased ability to cause MCF-7 cell proliferation.
      The uterotrophic activity of compounds was assessed with an Ishikawa (a human endometrial carcinoma cell line) cell stimulation assay using intrinsic alkaline phosphatase activity as a reporter (39, 40). Maximum alkaline phosphatase activity values were obtained for each compound (typically at concentrations greater than 1 μM), and these values were normalized to an estradiol control. For example, 4-OH tamoxifen, raloxifene, and GW7604 typically gave %E_{max} values of 14, 7, and 4 (41). Figure 7A shows Ishikawa data for a subset of compounds plotted *vs.* SRC-1(2) peptide binding (*blue squares*) for the same set of compounds. Data for five other peptides are also shown (*other colored symbols*).
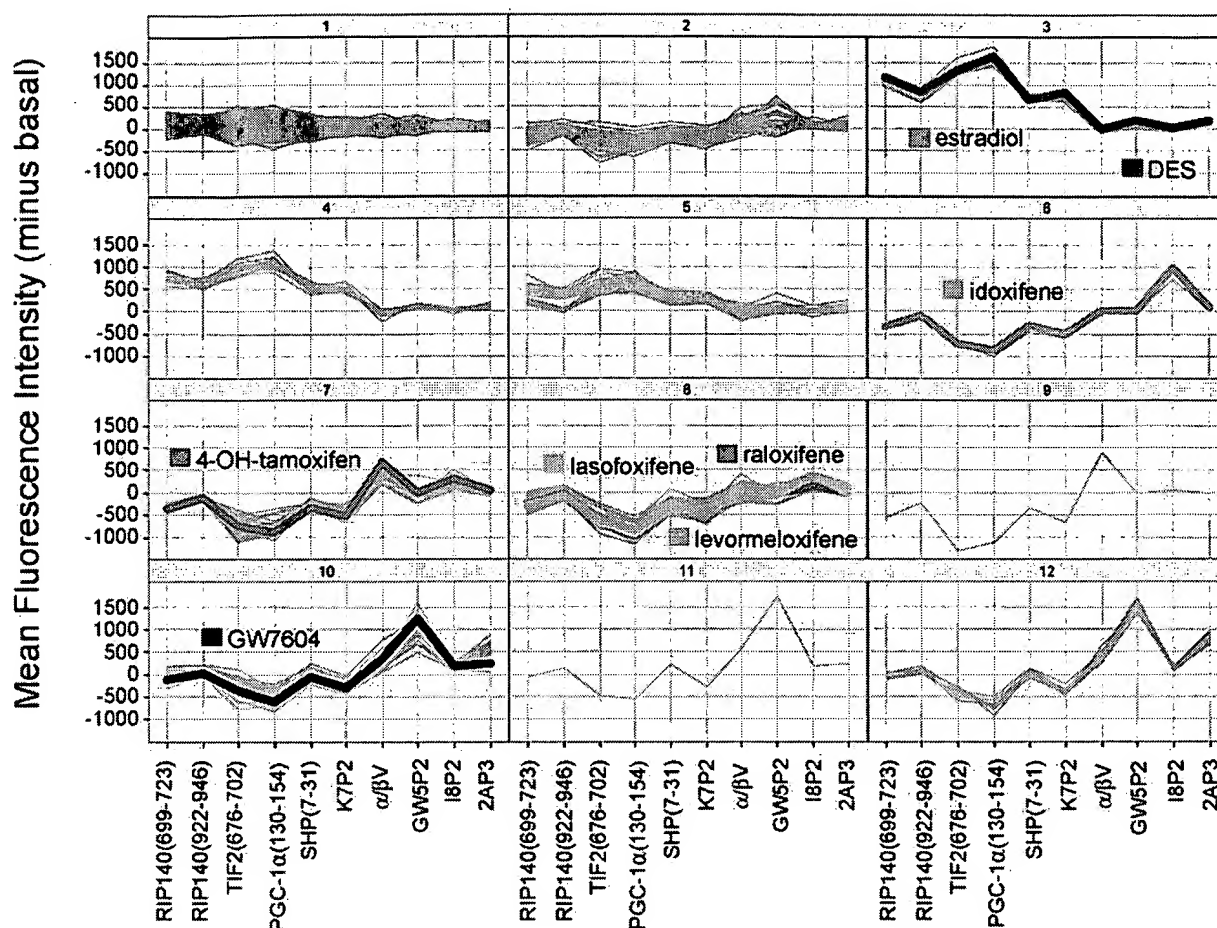
EXHIBIT T

Fig. 4. Categorization of ERα-Binding Compounds by Clustering of ERα LBD Peptide Binding Profiles

Profile plots of ERα LBD binding to peptides in the presence of various compounds are shown. Peptides shown are those chosen via the PCA-based method described in *Data Reduction Methods*. Profiles are grouped by shape-based cluster ID, which is represented in Fig. 3. Each *line* represents binding data for one compound where ERα LBD binding in the absence of compound has been subtracted. Each cluster contains peptide-binding data for one or more ERα compounds. The labels described in Fig. 2 identify profiles for tool SERM compounds.

Figure 7A shows that there is a general correlation between coactivator peptide recruitment and ability to stimulate Ishikawa cells. Figure 7B shows the relationship between Ishikawa stimulation and recruitment of three phage peptides, α/βV (tamoxifen-selective; *pink triangles*), I8P2 (idoxifene-selective; *cyan circles*), and GW5P2 (GW7604-selective; *yellow squares*). As shown, for compounds that showed significant recruitment of either the α/βV or I8P2 peptides, Ishikawa %E_{max} values were less than 20%. For compounds that recruit the GW5P2 peptide, the Ishikawa %E_{max} values were even lower (<5%).

In Figs. 5–7, we have shown that there is a general correlation between coactivator/phage peptide binding and the modulation of ER-driven cell-based activities imparted by these compounds. To further explore this relationship, Fig. 8 displays cell-based measurements for ERE, MCF-7, and Ishikawa assays in the same clusters as defined by the peptide binding data represented in Fig. 4. Figure 8 shows that, in general,

compounds that cluster together based on peptide profile also show similar cell-based activities. For several of the clusters, the cell-based data show highly consistent results within the cluster. For example, cluster 3 (with estradiol and DES) shows the expected high Ishikawa stimulation, MCF-7 proliferation and ERE activity. Cluster 7, containing 4-OH tamoxifen, shows low Ishikawa stimulation, MCF-7 proliferation and ERE activity. Compounds in cluster 10, which contains GW7604, show very low Ishikawa %E_{max} values (between 2 and 5%). Clusters 11 and 12, which like cluster 10 is defined by strong binding to the GW5P2-like peptides, also show a trend for low Ishikawa response. Compounds in cluster 8, which includes raloxifene, lasofoxifene, and levormeloxifene, yield relatively low Ishikawa %E_{max} values (between 5 and 20%) and show the ability to inhibit both MCF-7 proliferation and ERE activation.

Interestingly, for the compounds in clusters 1 and 2, where the peptide profiles were relatively flat, there did
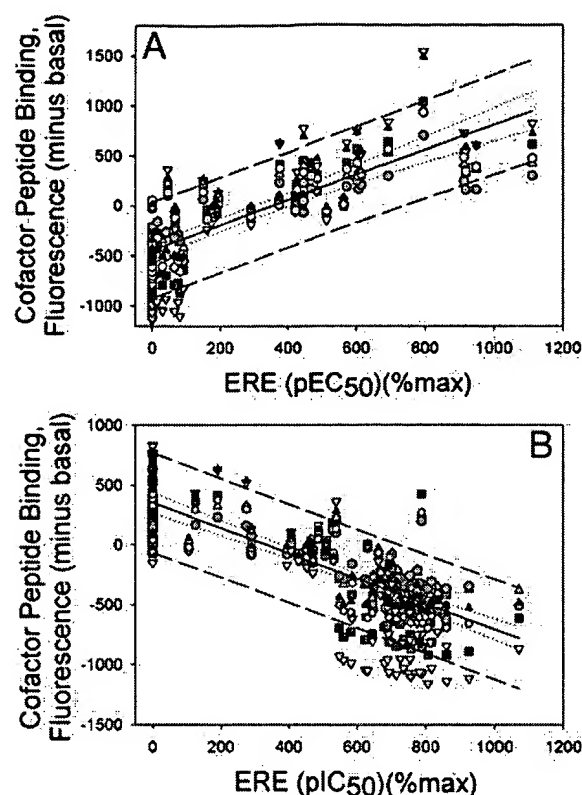
EXHIBIT T

Fig. 5. Effects of Compounds on ERE-Driven Reporter Gene Transcription as compared with ERα LBD Binding to Select Cofactor Peptides

ERα LBD peptide binding data were determined as described in Fig. 2. Each *point* represents binding data for one compound where ERα LBD binding in the absence of compound has been subtracted. Data for six peptides are represented by the following colors: SRC-1(2) (676–700) (*blue squares*), AIB1 (607–631) (*green triangles*), K7P2 phage derived (*red circles*), PGC-1α (130–154) (*yellow triangles*), DAX1 (132–156) (*cyan hexagons*), TIF2 (676–702) (*red triangles*). ERE data for the same compounds are plotted on the x-axis. The ERE assay was run in either (A) agonist or (B) antagonist mode as described in *Materials and Methods*. The %$_{max}$ values were determined by normalizing to either estradiol or raloxifene, respectively. The *solid line* indicates the best fit of all data points. The *dotted line* indicates 95% confidence interval and the dashed line is 95% prediction interval.

not appear to be much relationship among the cell-based data. Essentially, it appears that where there are no extreme positive or negative peptide descriptors for these compounds, these ligands can have a variable response in cells. One explanation for this is that our peptide interaction set does not contain enough interactors or descriptors to clearly differentiate compounds within these clusters. Also, cluster 5 shows heterogeneous cell-based responses. One attribute that clusters 1, 2, 5, and 8 have in common is the absence of a phage display peptide(s) to characterize the group. It is possible that additional phage-derived conformation sensing peptides could help in subcategorizing these clusters.
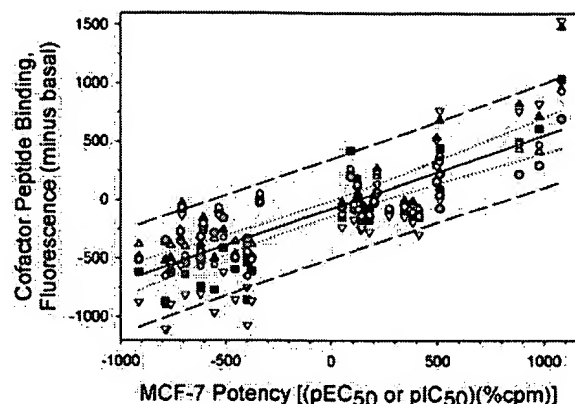

Fig. 6. Effects of Compounds on MCF-7 Cell Proliferation as Compared with ERα LBD Binding to Select Cofactor Peptides

ERα LBD peptide binding data were determined as described in Fig. 2. Each *point* represents binding data for one compound where ERα LBD binding in the absence of compound has been subtracted. Data for six peptides are represented by the following colors: SRC-1(2) (676–700) (*blue squares*), AIB1 (607–631) (*green triangles*), K7P2 phage derived (*red circles*), PGC-1α (130–154) (*yellow triangles*), DAX1 (132–156) (*cyan hexagons*), TIF2 (676–702) (*red triangles*). MCF-7 cell proliferation data for the same set of compounds are shown as an aggregate value incorporating both the pEC$_{50}$ or IC$_{50}$ and efficacy measurements. For %cpm determinations, data for all compounds were normalized to either estradiol (max) or raloxifene (min).

Correlation of Cell-Based Compound Effects with Corepressor Binding

Several recent studies have examined the role of an ERα:corepressor interaction in mediating the tissue-selective effects of tamoxifen and raloxifene (42–44). We used the 405 compound set to search for ligands that might enhance the interaction between ERα LBD and a peptide derived from either nuclear hormone receptor corepressor (NCoR) or silencing mediator of retinoic acid and thyroid receptor (SMRT). As shown in Fig. 9, A and B, a number of compounds were shown to enhance the recruitment of both the NCoR 1 [amino acids (aa) 2040–2065] and SMRT 2 (aa 2329–2354) peptides. The compounds that were most successful at enhancing this interaction are those with an acrylate or carboxylate head group extension (like GW7604; shown as *green squares*). In addition, some novel head groups were also found to induce the same response and cluster with the acrylate-containing compounds (*red squares*). As shown in the two examples in Fig. 9, the same compounds that increased corepressor peptide binding also increased binding to the GW5P2 phage display peptide and the GW5P2-like peptide, 47P3.

Examination of the peptide sequences found with the ERα:GW7604 complex revealed that these pep-
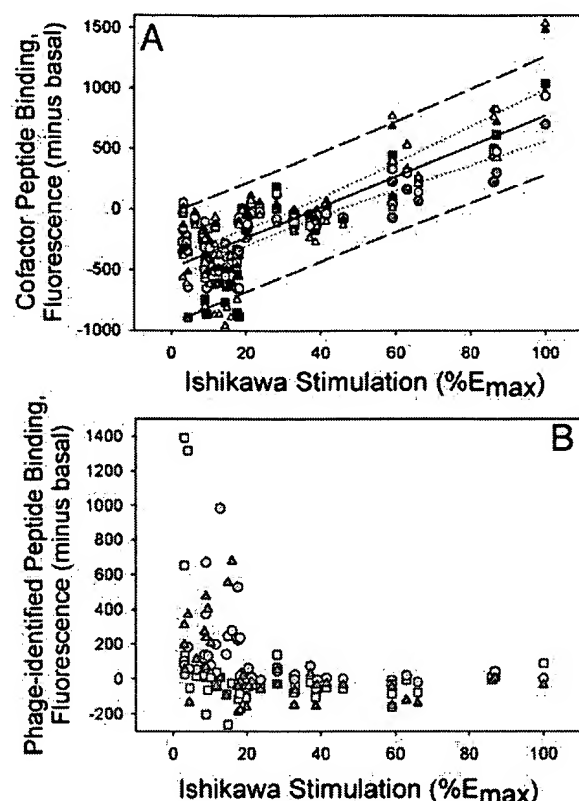
EXHIBIT T

Fig. 7. Effects of Compounds on Ishikawa Cell Stimulation as Compared with ERα LBD Binding to Select Cofactor Peptides

ERα LBD peptide binding data were determined as described in Fig. 2. Each set of *points* represents binding data for one compound where ERα LBD binding in the absence of compound has been subtracted. Ishikawa cell stimulation data are shown for the same set of compounds. For the Ishikawa %E_{max} value, each compound was normalized to a standard estradiol stimulation curve (100%). A, SRC-1(2) (676–700) (*blue squares*), AIB1 (607–631) (*green triangles*), K7P2 phage derived (*red circles*), PGC-1α (130–154) (*yellow triangles*), DAX1 (132–156) (*cyan hexagons*), TIF2 (676–702) (*red triangles*). B, GW5P2 phage display peptide (*yellow squares*), I8P2 phage display peptide (*cyan circles*), α/βV phage display peptide (*pink triangles*).

tides share the same hydrophobic residue spacing as corepressor motifs (Fig. 10). This alignment shows that the typical corepressor motif of LXX(H/I)IXXX(L/I) is represented in the majority of the acrylate-sensing phage display peptides. In addition, a Leu at the −1 position and the basic amino acid at the +7 position were selected in both the primary random 10-residue peptide library and the second-generation GW5P2-based library. Selection from the latter library identified a Thr at the −2 position and a Leu at the −3 and +12 position to further extend the presumed amphipathic helix. Also, Phe and Trp were preferentially selected at the +1 and +5 positions, where the corepressor contains the smaller hydrophobic amino acids Leu and Ile, respectively.

DISCUSSION

The search for novel ERα ligands has previously relied heavily on cell-based predictive assays. A number of studies, using protease digestion (45), crystallography (12, 46), and phage display (28, 29), have elegantly shed light on the molecular mechanism for ligand-induced receptor conformations for ERα. Such studies have highlighted the importance of receptor dynamics in governing outcomes of ER-binding compounds. An important step in further understanding the details of ERα signal transduction and the consequent discovery of new modulating ligands is further defining the link between receptor conformation and biological activity of SERMS. Here, we have used various ERα-binding small molecules as tools to probe both receptor conformation, via peptide interactions, and cell-based activity. In general, these results show that peptide interaction profiles correlate well with, and could be used to predict, the biological consequence of ligand binding within a cell as described by a set of cell-based predictive assays. These correlations further highlight the dominant role that ligand-induced conformation and association with cofactor have on ERα cellular function.

There has been tremendous effort toward understanding the differential effects of SERMs and the effects that they cause at the cellular level (17). One approach has been to use differential gene expression to fingerprint and classify ER ligands based on their ability to alter RNA transcript levels (47, 48). It is becoming clear from these types of studies that gene expression patterns help explain why some ER-modulating ligands display both beneficial outcomes and undesired activities such as activity in uterine or breast tissue. Future work should allow assigning specific genes to particular biological effects elicited by SERMs, such as retention of bone mineral density (49). However, parsing through the enormous numbers of available and newly synthesized ER-binding compounds at the cellular level is a daunting task. The results presented here demonstrate that the ligand-induced conformation of ER can be probed through protein-peptide interactions and these binding profiles may be used to characterize and bin new SERMs to aid selection of novel compounds. Compounds that yield profiles unlike those of known SERMs can be rapidly identified and flagged for further cell-based or animal-based work. This relatively high-throughput technology should help guide ER and other nuclear receptor chemistries for fine-tuning modulators of the future.

Interestingly, we have made these *in vitro* to cellular correlations even though our multiplexed peptide binding assay uses purified LBD. In fact, our ERα expression construct contains an abbreviated form of the LBD (aa 299–554) that deletes the extended strand after the AF helix (F domain). Although we observe excellent correlations, expanding efforts to include
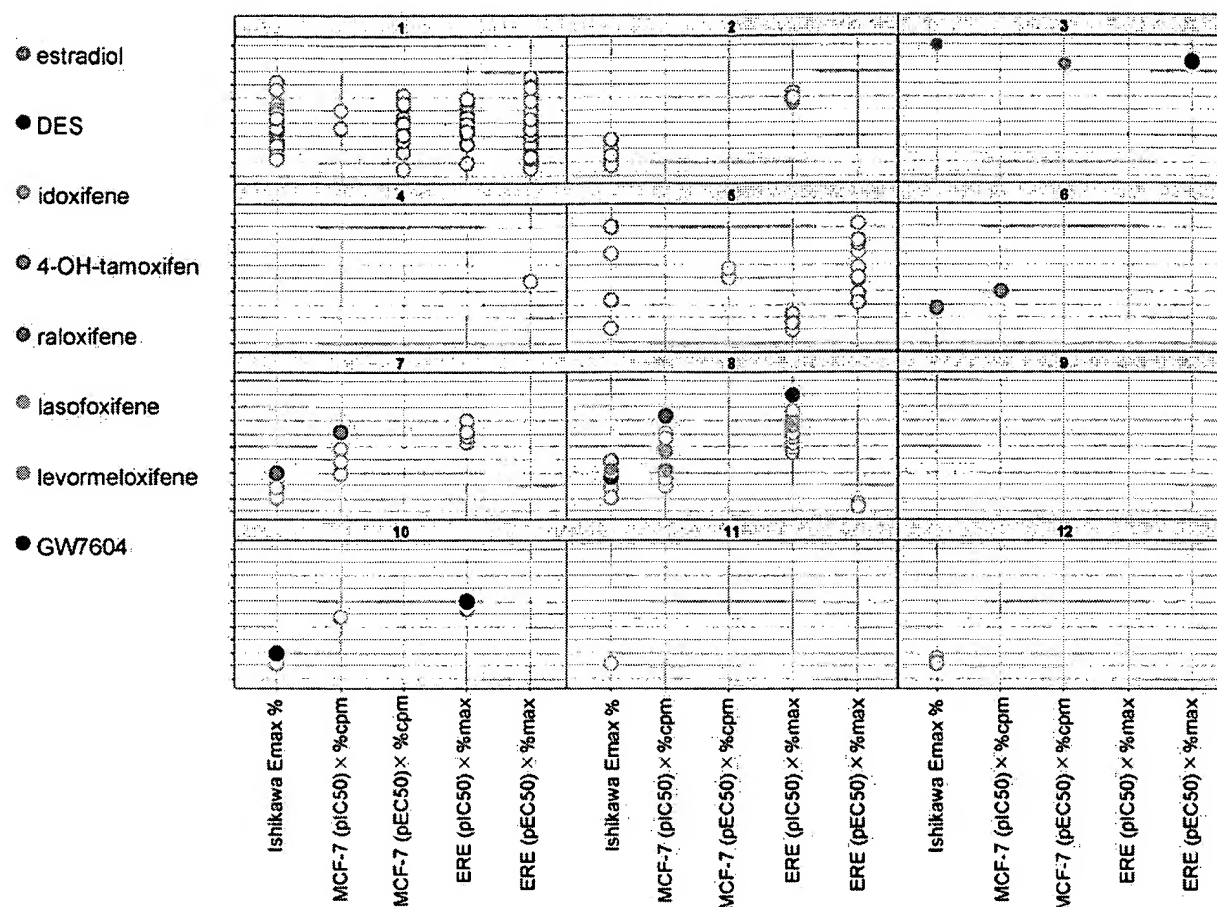
EXHIBIT T

Fig. 8. Relationship of Cellular Data to ERα LBD Peptide Binding Profiles for ERα-Binding Compounds by Clustering

Cell-based assay data for Ishikawa, MCF-7, and ERE are shown in each cluster as organized by peptide profile characteristics. Cell-based data were generated as described in Figs. 5–7 and *Material and Methods*. Clusters 1–12 were determined based on the ER α LBD peptide profiles described in Fig. 4A. Each *point* represents cell-based data for one compound and each cluster is based on peptide-binding data for one or more compounds. Cell-based data for tool SERM compounds are coded as follows: estradiol (*blue-green*), DES (*dark blue*), 4-OH tamoxifen (*red*), GW7604 (*black*), idoxifene (*green*), levormeloxifene (*light blue*), lasofoxifene (*blue*), and raloxifene (*pink*). Other compounds tested are shown as *gray open circles* in the background. The scale for the cell-based values is as follows: Ishikawa E%$_{max}$, 0 − 100%; MCF-7 pEC$_{50}$ × %cpm, 0 − 1000; MCF-7 pIC$_{50}$ × %cpm, 0 − 1000; ERE pEC$_{50}$ × %$_{max}$, 0 − 1000; ERE pIC$_{50}$ × %$_{max}$, 0 − 1000.

full-length receptor and peptide/protein/DNA binding partners that recognize other regions of ER (such as the AF-1/DNA-binding domain/hinge regions) should increase the amount of information garnered. It is well documented that ERα has numerous activities driven through the N-terminal AF1 domain. For example, it has been shown that the AF1 domain is phosphorylated upon ligand binding and that other ligand-induced activities can occur via cytoplasmic signaling events (50). The relationships that we derive in this current study demonstrate that ligand-influenced AF2 function is a dominant feature of ERα signal transduction, and it is likely that AF1 phosphorylation and its activities are linked to the AF2 in the context of the full-length receptor. Although our data suggest that most of the receptor function correlates with ligand-dependent AF2 function, it is important to consider the possibility that *in vitro* profiling may not completely correlate with ERα LBD binding and function. A case

could be made that nongenomic effects, possibly driven through an alternate signal transduction pathway such as recently shown for progestin (51), may yield discrepancies between LBD profiling and cell-based activities for ERα ligands. Additionally, lack of correlation between peptide binding characteristics *in vitro* and the effect of compounds on a cell could be due to lack of cell penetration by a compound or due to metabolic alteration of a compound upon entering a cellular environment.

Although a number of studies have suggested differential coactivator recruitment by ERα ligands (52, 53), we have found, under our experimental conditions, that binding characteristics for most cofactor-derived LXXLL peptides track with one another. Generally, all estradiol-like compounds proportionally increased LXXLL peptide binding relative to basal binding and all tamoxifen- or raloxifene-like compounds proportionally decreased LXXLL binding. Ap-
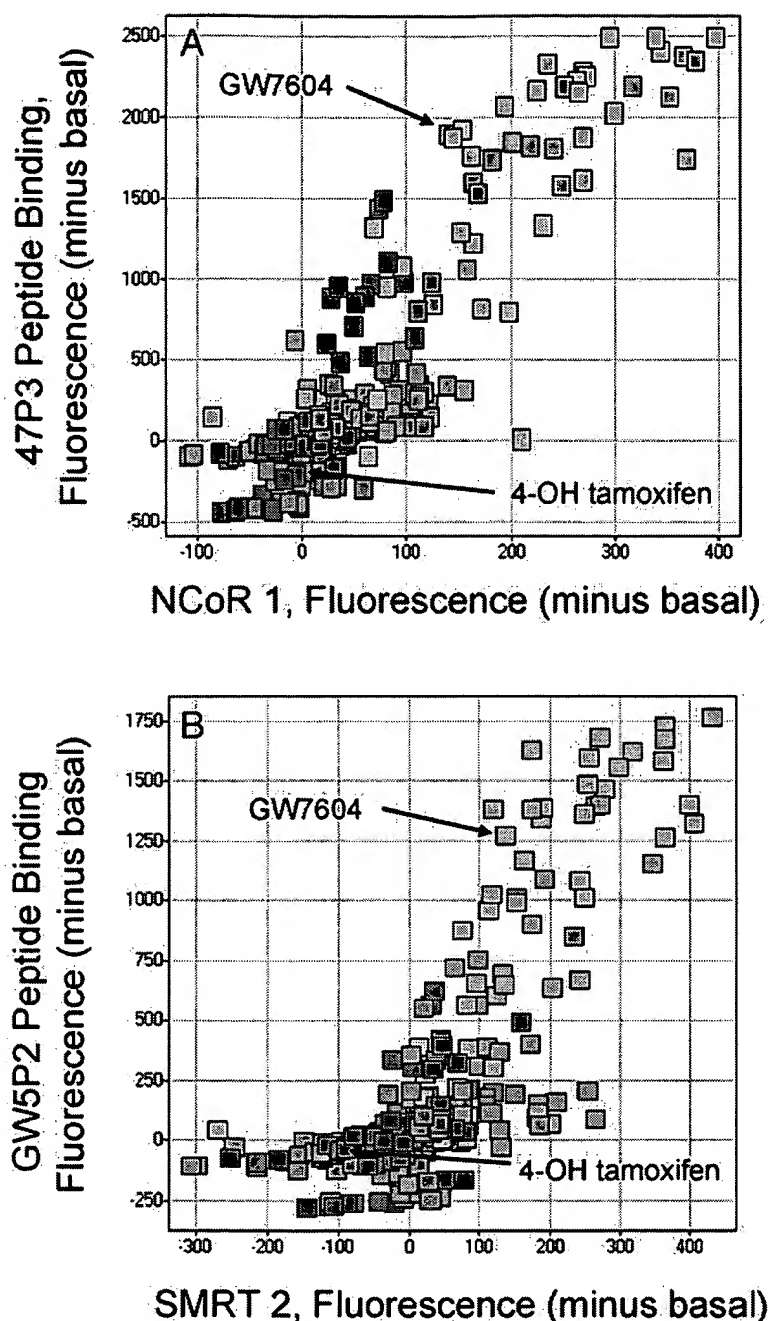
EXHIBIT T

Fig. 9. Comparison of Compound Effects on ERα LBD Binding to Phage Display and Corepressor Peptides

    Binding of compound-bound ERα to the respective peptide was measured using fluorescent microspheres and flow cytometry as described in *Materials and Methods* and Fig. 2. Each *point* represents binding data for one compound where ERα LBD binding in the absence of compound has been subtracted. The three colors represent different classes of compounds: *green* depicts compounds that contain either an acrylate or carboxylate head group (GW7604 is one example), *blue* depicts compounds that contain a tertiary amine head group (4-OH tamoxifen is one example), and *red* shows those compounds with a unique head group. A variety of different core scaffolds are represented in addition to the triphenylethylene.

plication of PCA deselected 39 of the 44 cofactor peptides used in this study. In other words, the five cofactor peptides shown in Fig. 2C were adequate to fully describe the compound-induced binding trends of all cofactor peptides. It is possible that very subtle differences in cofactor recruitment with various com-

pounds may require full-length proteins, where sites distal to the coactivator cleft (on the receptor) and/or NR box (on the cofactor) may play a role. Clearly though, as noted by previous studies (54, 55), there are distinct LXXLL preferences for ERα LBD where, as shown in Fig. 2, A and B, peptides from RIP140,

EXHIBIT T

Peptide

```
GW5P2        E D G G S L F E R V W L R E L G
47P3     E D G G S A L T L F D R V W L R E H Q P L G
33P4     E D G G S V L T L F E R V W L R E L S C L G
2AP3       E D G G S P L W Q I F S R E L G
7β-16        H F L I N Q H L Y K L L Q D T D I V V
NCoR 1     H R L I T L A D H I C Q I I T Q D F A R
NCoR 2   P A S N L G L E D I I R K A L M G S F
SMRT 1     Q R V V T L A Q H I S E V I T Q D Y T R
SMRT 2   H A S T N M G L E A I I R K A L M G K Y
```

```
                 -2 -1 +1              +7
Consensus        φ X L X X φ φ X R X φ
                   P              K
```

Fig. 10. Alignment of Phage Display Peptide Sequences with NCoR and SMRT Interaction Motifs

The peptides identified using random peptide phage display against ERα complexed with GW7604 or other acrylate head group compounds are shown aligned with the corepressor binding motifs from both NCoR and SMRT. The phage display peptides are GW5P2, 2AP3, 47P3, 33P4, and 7β-16 [which was identified by Connor *et al.* (59)].

SRC-1, TIF2, AIB1, PGC-1α, SHP, and DAX yield the highest binding signal. It is interesting to note that four of these five peptides, in addition to the phage-derived peptide K7P2 (*LLRWYL*), show a weak sequence relationship of φ *LKXLL*, where φ represents a hydrophobic side-chain (Leu, Val, or Ile) and K represents Lys in addition to the other basic residues Arg, Gln, and His (Table 1) (56). The DAX peptides deviate slightly by containing a Tyr residue at the +2 position (*ILYXM/LL*). These peptide sequences, notably K7P2, DAX (66–90), and DAX (132–156), also suggest that ERα is able to tolerate either a Met or Tyr in the +4 position. A full understanding of the detailed molecular recognition aspects of the preferential binding of certain peptides will require further structural and functional analysis.

Figures 5–7 show that there is a consistent relationship between compound-induced coactivator peptide recruitment and the effect of compound on ERα-driven cell response. To more accurately show this correlation, we have assembled various cell-based activities for a subset of the tool compounds and organized these data into clusters based on similarity of peptide profiles (Fig. 8). As shown, most of the cell-based data are similar in each particular cluster. The most obvious exceptions are data shown in cluster 1. The peptide profiles for this cluster are relatively unchanged from the peptide profile of ERα in the absence of compound (*i.e.* the change in relative fluorescent intensity is approximately zero for all peptides). Although the compounds in this cluster bind with relatively high affinity, they do not appear to induce a unique, stabilized conformation. These types of ligands may act as competitive antagonists by keeping the receptor in an apo-like state. In this situation, the ligand-bound LBD structure would be predominantly a dynamic state similar to the ligandless receptor. It will be interesting to pursue whether or not peptides or other binding partners will be able to further discriminate compounds that appear to induce a

somewhat neutral conformation. With additional peptides, the correlation of peptide profile with cellular activity for ligands within this cluster may improve.

It has been noted that tamoxifen, although developed as an antiestrogen for the treatment of breast cancer, has estrogenic activities in certain tissues (57). In particular, tamoxifen exhibits minimal, but significant uterotrophic activity relative to raloxifene. With respect to the LXXLL cofactor peptides, both tamoxifen and raloxifene induce very similar peptide profiles (Fig. 2B). However, the binding profiles are clearly distinct with respect to the tamoxifen-selective peptide α/βV (29) (Fig. 2C). Interestingly, compounds that induce recruitment of the peptide also yield an Ishikawa stimulation value less than 20% (Fig. 7B). One explanation for this relationship may be that the tamoxifen-selective peptide represents an uncharacterized cofactor that may be expressed in uterine tissue but not breast tissue. Although it has been demonstrated by chromatin immunoprecipitation experiments (44), we were not able to detect a significant difference with SRC-1 peptide recruitment between tamoxifen and raloxifene *in vitro*. This may be related to a lack of an AF1 region on ERα or lack of full-length SRC-1 cofactor as regions outside the LXXLL may play a partial role in recruitment. In addition, we were not able to detect a significant interaction between ERα and corepressor peptide with either tamoxifen or raloxifene.

To even further discriminate compounds with low uterine stimulatory activity via peptide profiling, we have selected peptides specific for two compounds, idoxifene and GW5638, or its 4-hydroxyl version GW7604. These compounds yield Ishikawa stimulation values less than 15% relative to estradiol. As shown in Fig. 2, B and C, the two selected peptides, I8P2 and GW5P2, are specifically recruited to ERα upon binding of idoxifene or GW5638/GW7604, respectively. In addition, our test compound set contains several molecules similar to idoxifene and

EXHIBIT T

GW5638/GW7604 and these compounds also induce recruitment of the selective peptides (Fig. 2C). Similar to the α/βV tamoxifen-selective peptide, comparison of I8P2 and GW5P2 peptide recruitment with Ishikawa cell stimulation, shows that compounds that induce ERα binding to these peptides also exhibit uterine cell activity approximately less than 20% (Fig. 7B). From the comparison of peptide and Ishikawa activities, the GW5P2 peptide appears to predict an even lower uterine activity. Although only several compounds are shown, we have examined more than 15 compounds that induce recruitment of the GW5P2 peptide and all these compounds display an Ishikawa activity less than 5% relative to estradiol (data not shown).

Sequence alignment shows that there is a relationship between the set of phage peptides isolated against the ERα:GW5638/GW7604 complex and the corepressor peptides, from both NCoR and SMRT (Fig. 10). Compound-induced recruitment shows that both these phage peptides and the corepressor peptides are recruited by same compounds in a linear relationship (Fig. 9, A and B). This suggests that these peptides may interact at the same site on ERα and have the same mode of interaction with ERα. It is possible that the GW5P2 and 47P3 peptides identified by phage display are affinity-optimized versions of corepressor peptides. If this is the case, the hydrophobic face of the amphipathic helix would be approximately one helical turn longer than the typical coactivator peptide and the interaction on the receptor would require repositioning of the AF helix as shown in the recent peroxisome proliferator-activated receptorα/SMRT peptide crystal structure (58). As shown in Fig. 9, the binding signal for the GW5P2 and 47P3 phage peptides is approximately 3- to 5-fold higher than that for the corepressor peptides. One possibility for the increased signal (due to increased affinity) is that the selected Phe at +1, Val at +4, and Trp at +5 provide more hydrophobic surface area for packing against the extended corepressor cleft. It is interesting that the acrylate head group compounds optimally create this molecular recognition surface on ERα. Using an LXXLL focused library, Connor *et al.* (59) also identified a similar peptide consensus from phage display results with ERα:GW7604. Further structural and functional work will be required to elucidate the precise molecular recognition of these peptides and relevance of their similarity to the corepressor motif. From this example, and the fact that phage display peptides contribute a large degree of the prediction information for peptide profiling, it appears that the selected peptides might represent naturally occurring protein partners, some of which may remain to be discovered.

As mentioned briefly above, the compound-selective peptides offer a great deal of diversity to the peptide-binding profiles in this type of approach. For examining new ligands, the profiles can give clues that a new ligand is unique compared with tool compounds, even if a specific peptide for that new ligand

is not in the peptide set. In fact, compounds that induce either novel or neutral profiles can be selected for further random peptide work to identify new peptides to add to the screening set. In contrast to a static picture provided by a crystal structure, this type of profiling analysis provides a sense of the activities of the receptor, which is a balance between various "on" and "off" states. In effect, the peptide interaction profile is sensitive to the dynamics of the receptor when bound with ligand.

Much of the detail for how ligand-induced receptor dynamics translates to signal transduction capacity in a cellular environment has yet to be completely defined. Our data add to the mounting evidence that the allosteric coregulator recruitment activity of ERα, as well as other members of the nuclear receptor family, is a dominant feature of receptor function that ultimately links biological activity to the ligand. Visualization of the multitude of ligand-induced peptide profiles further emphasizes the structural and functional plasticity of the nuclear receptor LBD. Understanding how to manipulate the numerous pathway activities of ERα with ligands, even with many current unknown factors, remains a goal for both drug and tool compound discovery. This microsphere-based compound profiling strategy, coupled with random peptide library technologies, can be a valuable tool to rapidly assess compound-induced conformations of ERα and can aid in the early identification of unique potential drug candidates.

MATERIALS AND METHODS

Protein

The ligand binding domain of ERα was expressed in *Escherichia coli*, purified to homogeneity, and biotinylated similar to that described previously for ERβ LBD (25). The expression construct consisted of aa 299–554 and mass spectrometry was used to verify the mass of the purified protein. Full-length ERα was purchased from Invitrogen (Carlsbad, CA).

Selection of ERα-Binding Compounds

All compounds were either synthesized in the GlaxoSmithKline Medicinal Chemistry Laboratories or were purchased from commercial sources. Solid compounds were dissolved in dimethylsulfoxide (10 mM) and subsequently diluted with buffer before use. An *in vitro* [³H]estradiol displacement assay was used to select ERα-binding compounds from a large set of candidate compounds (data not shown). The compounds selected for further analysis in the microsphere-based peptide binding assay and the cell-based assays had pK_i's > 6. The average pK_i for the 405 compounds in this test set was 7.2 with SD of 0.8. The compound set included several classic, well-characterized ERα ligands such as estradiol, DES, raloxifene, 4-OH tamoxifen, idoxifene, levormeloxifene, lasofoxifene, and GW7604 (35) (Fig. 1).

Phage Display

A modified polyvalent phage display vector, fGWg3, was constructed using the original vector fTC (60). fGWg3 con-

EXHIBIT T

tains a flag tag epitope (AspTyrLysAspAspAspLys) in frame immediately upstream of the sequence for the M13 geneIII protein. This vector was also engineered to contain a dual *Bbs*I site between the signal sequence of the M13 gene III and the flag tag. A random peptide library, fGWX10, was constructed by inserting a DNA cassette containing ten consecutive NNK codons, where N represents an equal molar ratio of A, C, G, and T and K represents G and T, into *Bbs*I digested fGWg3. This library displays a random 10-residue peptide sequence with flanking regions as follows: NH2-EDGGSX$_{10}$(GGGGS)$_3$-gIII protein. The DNA cassette encoding the random peptide sequence was constructed using a synthetic ligase chain reaction procedure (61) with the following four oligonucleotides: 5'-TGGGTCCIII IIIIIIIII IIIIIIIII IIIIIIGGA GGCGGGGGTA-3', 5'-GCGGCGGTGG AGGGT-CTGGG GGAGGTGGCT CTGGGAAGAC CT-3', 5'-TTCC-AGGTCT TCCCAGAGCC ACCTCCCCCA GACCC-3', and 5'-TCCACCGCCG CTACCCCCGC CTCCMNNMNN MNNM-NNMNNM NNMNNMNNMN NMNNGGA-3', where I represents inosine, M represents equal molar of C and A, N represents equal molar of A, C, G, and T. *E. coli* MC1061 cell electroporation and phage library preparation have been described previously (62). After ligation and transformation, a small fraction of the library was plated on LB/tetracycline plates. The library contained approximately 10^{10} transfor-

mants and individual clones were analyzed by both DNA sequencing and phage ELISA using immobilized anti-Flag monoclonal antibody.

A second-generation phagemid display library was constructed based on the selected peptide sequence for ERα plus GW5638 (Table 1). The library oligonucleotide was made to re-randomize the nucleotide sequence encoding the GW5638 selected peptide. An oligonucleotide for cassette mutagenesis was synthesized with base mixtures where each base position was fixed at 80% based on the original template sequence and an equal mixture of the three other bases was used at 20%. In addition, three NNS, where S represents an equal molar ratio of G and C, randomized codons were added to both ends of the re-randomized oligo segment. This oligonucleotide mixture sequence served as a template for PCR amplification using the following sequences as primers: 5'-ccg gcc atg gcc gaa gac ggt ggg-3' and 5'-tac cag gtt cca ggt ctt ccc aga gcc acc tcc ccc aga ccc tcc acc gcc gct acc ccc gcc tcc-3'. The PCR amplified cassette was ligated into a *Bbs*I-digested, gel purified pGW BBS6g3 phagemid vector. The ligated library was electroporated into XL1-Blue cells and titered to yield 1.25 × 10^9 individual transformants. Random clones were selected and analyzed by DNA sequencing to show that 94% of the clones had correct inserts containing randomized DNA sequences.

Table 1. Peptide Sequences Used to Profile ERα-Modulating Compounds

Peptide	Amino Acid Residues[a]	Sequence
Phage Display Peptides		
K7P2	NA	EDGGSLLRWYLEHEFGGGGSGK (Ahx-B)[b]-CONH$_2$
α/βV[c]	NA	SSPGSREWFKDMLSRGGGGSK (Ahx-B)-CONH$_2$
I8P2	NA	EDGGSWVEWVEEERRGGGGK (Ahx-B)-CONH$_2$
R5P2	NA	EDGGSRRFTFQYGSV (GGGGS)$_3$GK (Ahx-B)-CONH$_2$
2AP3	NA	EDGGSPLWQIFSRELGGGGSK (Ahx-B)-CONH$_2$
GW5P2	NA	EDGGSLFERVWLREL (GGGGS)$_3$GK (Ahx-B)-CONH$_2$
47P3	NA	QPAMAEDGGSALTLFDRVWLREHQPLGGGGSK (Ahx-B)-CONH$_2$
33P4	NA	QPAMAEDGGSVLTLFERVWLRELSCLGGGGSK (Ahx-B)-CONH$_2$
7β-16[d]	NA	ASRHFLINQHLYKLLQDTDIVVSRLGGGGSK (Ahx-B)-CONH$_2$
Coactivator Peptides[e]		
RIP140	699–723	B-SGSEIENLLERRTVLQLLLGNPTKG-CONH$_2$
RIP140	922–946	B-EHRSWARESKSFNVLKQLLLSENCV-CONH$_2$
TIF2	676–702	B-GSTHGTSLKEKHKILHRLLQDSSSPVD-CONH$_2$
TRAP 220	590–614	B-GHGEDFSKVSQNPILTSLLQITGNG-CONH$_2$
TRAP 220	631–657	B-PVSSMAGNTKNHPMLMNLLKDNPAQ-CONH$_2$
RAP250, PRIP	874–898	B-FPVNKDVTLTSPLLVNLLQSDISAG-CONH$_2$
RAP250, PRIP	1476–1500	B-NKNLVSPAMREAPTSLSQLLDNSGA-CONH$_2$
PPARγ CoA-1 α	130–154	B-DGTPPPQEAEEPSLLKKLLLAPANT-CONH$_2$
Coregulator Peptides		
SHP	7–31	B-ACPCQGAASRPAILYALLSSSLKAV-CONH$_2$
SHP	104–128	B-VTFEVAEAPVPSILKKILLEEPSSS-CONH$_2$
DAX	1–23	B-MAGENHQWQGSILYNMLMSAKQT-CONH$_2$
DAX	66–90	B-CCFCGKDHPRQGSILYSMLTSAKQT-CONH$_2$
DAX	132–156	B-CCFCGEDHPRQGSILYSLLTSSKQT-CONH$_2$
Corepressor Peptides		
NCoR 1	2040–2065	B-GQVPRTHRLITLADHICQIITQDFAR-CONH$_2$
NCoR 2	2251–2275	B-GHSFADPASNLGLEDIIRKALMGSF-CONH$_2$
SMRT 1	2124–2149	B-PGVKGHQRVVTLAQHISEVITQDYTR-CONH$_2$
SMRT 2	2329–2354	B-SQAVQEHASTNMGLEAIIRKALMGKY-CONH$_2$

[a] As specified in GenBank.
[b] Ahx-B represents 6-aminohexanoic acid-biotin conjugate.
[c] Sequence reported in Ref. 29.
[d] Sequence reported in Ref. 59.
[e] See Ref. 25 for other coactivator peptide sequences.
NA, Not applicable. *Boldfaced letters* in the peptide sequences represent consensus residues in coactivator and corepressor peptides.

EXHIBIT T

In preparation for selection of specific peptide clones, 500 nM of either biotinylated ERα LBD or biotinylated ERα FL in the presence of 1 μM compound of interest was immobilized on a neutravidin-coated microtiter plate well. Protein was immobilized for at least 1 h at room temperature and then wells were washed three times with PBS. For the first round of selection, approximately 10^{12} phage particles were added in casein blocking buffer (0.89 g dibasic sodium phosphate, 2.5 g Hammarsten casein, and 2.9 g sodium chloride in 250 ml ddH$_2$O) plus the compound of interest. Phage were allowed to bind for 2 h at room temperature. After washing with PBS/0.025% Tween 20 to remove unbound phage, bound phage were eluted with 0.1 N HCl plus 1 mg/ml BSA, the solution in the well was adjusted to pH 2.2 with glycine and then neutralized with 2 M Tris-HCl. An aliquot of the eluted and neutralized phage was added to 1 ml of confluent K91 cells. Cells were infected with phage particles for 15 min at 37 C, and then cultures were grown overnight at 37 C. The following day, phage were harvested by standard methods using 10% polyethylene glycol-8000/2.5 M NaCl in preparation for the next round of selection.

After each round of phage sorting, eluted phage were titered to determine population enrichment. Typically after two to three rounds of selection, enrichment was observed and individual clones were analyzed by DNA sequencing. Phage ELISA (63) was used to assess both peptide affinity for immobilized ERα and the selectivity of the peptide for the receptor in the presence of ligand. Based on phage ELISA signal and selectivity *vs.* a panel of known SERMs, individual peptides were chosen for synthesis.

Synthetic Peptides

Biotin-containing peptide sequences derived from coactivator, corepressor, and coregulator proteins or identified by phage display were synthesized by the Synpep Corp. (Dublin, CA), or American Peptide Co. (Sunnyvale, CA). Each peptide was purified by reverse-phase HPLC. Amino acid composition and peptide concentration were determined by conventional methods for each peptide sequence. Typically, these peptides were biotinylated during synthesis at the ε-amino group of lysine of the G$_4$SK C terminus. This orientation allows for attachment to a solid support similar to the direction displayed as a gIII fusion. Some of the peptides, such as R5P2 for raloxifene and 30P2 for GI5986, did not display high signal-to-background (at 10 nM ERα LBD) as synthetic peptides relative to signal achieved with phage ELISA. It is possible that these peptides require some aspect of the gIII protein or some other phage coat protein as structural scaffolding to allow display of active peptide on phage, whereas the pure synthetic peptide is not active. Therefore, these weaker affinity synthetic peptides were not typically useful in the multiplexing format used in this report (see below). An alternative for future consideration is that the peptide binding site density on the surface of the microsphere can be tailored according to the affinity so that both high and lower affinity peptides can be used in the same multiplexed experiment (25).

Fluorescent Microspheres

Lumavidin-coated polystyrene microsphere populations (5.6 μm in diameter) with 10^6 biotin-binding sites per bead were purchased from the Luminex Corp. (Austin, TX).

Coupling of Biotinylated Peptides to Microspheres

Each biotinylated peptide was coupled to a specific population of microsphere as described previously (25). Briefly, in 96-well 1.2-μm filter-bottom plates (Millipore, Bedford, MA), Lumavidin-coated microspheres were washed in buffer (PBS containing 0.02% Tween 20, 0.1% BSA, 0.02% sodium azide and 1 mM dithiothreitol) and incubated with biotinylated peptide (2.0 μl of a 100 μM stock) for 30 min at room temperature in the dark. An additional 30-min incubation with free D-biotin (20 μl of 5 mM D-biotin) was conducted to stop the coupling reaction and block any unoccupied biotin-binding sites. The microspheres were washed twice, combined and resuspended in buffer. Quantitation of the coupling reaction was determined by flow cytometry as described previously (25). All peptide couplings were evaluated to assure that peptide density was at least 250,000 peptide molecules per microsphere. We have determined previously (25) that this peptide density minimizes the variation due to avidity or rebinding effects. The microsphere populations were coupled on the day of the binding experiment.

Coupling of ERα LBD to Fluorochrome

The coupling of ERα LBD to the reporter fluorochrome Alexa 532 (Molecular Probes, Eugene, OR) was performed essentially as described previously (25). Briefly, purified, biotinylated recombinant ERα LBD was incubated with Strepavidin Alexa 532 at a 10:1 molar ratio of receptor to fluorochrome for 2.0 min. The coupling reaction was stopped by adding 20 μl free D-biotin (5 mM) and incubating for 30 min at room temperature in the dark.

Multiplexed ERα LBD Binding Assay

All components (microspheres, ligand, Alexa 532-labeled ERα LBD) were combined in the wells of a 96-well microtiter plate in a total volume of 75 μl. Each microtiter well contained 3,000 microspheres of a given population and up to 60 individual microsphere populations. The suspensions incubated for 1.5–2 h at room temperature in the dark. Fluorescence associated with each microsphere was directly measured by flow cytometry without washing.

Microsphere-associated fluorescence was measured using a LX-100 flow cytometer (Luminex Corp., Austin, TX) equipped with an XY platform for automated sampling from the wells of a 96-well microtiter plate. The LX-100 has two lasers. The red laser (633 nm) excites the fluorochromes embedded within the microsphere for population identification and the green laser (532 nm) excites the reporter fluorochrome on the nuclear receptor to indicate binding. Instrument calibration was conducted using LX-100 calibration microspheres purchased from the Luminex Corp. according to the manufacturer's instructions. Microsphere fluorescence was determined per well from a minimum of 100 microspheres of each microsphere population and was gated to exclude doublets and aggregates using side scatter measurements. Microsphere populations were identified by their unique two-dimensional fluorescent profiles at 658 and 712 nm. ERα LBD binding was measured at 575 nm and is represented in relative MFI units.

ERE Assay

The ERE assay was conducted by transiently transfecting a T47D breast cell line with a plasmid containing 1) the frog vitellogenin promoter which drives expression of a secreted placental alkaline phosphatase reporter gene, and 2) a plasmid that expresses the full-length ERα gene. The vitellogenin promoter contains the consensus vitellogenin ERE sequence (F-vitERE) (36, 64). In this ERE assay, the presence of an ERα agonist increases transcriptional activity of the reporter gene. Compounds were evaluated for their potential to either stimulate transcriptional activity (agonist mode, increasing concentrations of compound are incubated with cells in the absence of a competing compound) or inhibit transcriptional activity (antagonist mode, increasing concentrations of compound are incu-

EXHIBIT T

bated with cells in the presence of a fixed concentration of estradiol). Transcriptional activity was measured by acquisition of OD_{405} which indicates secreted placental alkaline phosphatase activity. An EC_{50} (agonist mode) or IC_{50} (antagonist mode) was determined for each compound tested. A compound's ERE potency is defined as $pEC_{50} \times \%_{max}$ (agonist mode) or $pIC_{50} \times \%_{min}$ (antagonist mode).

MCF-7 Cell Proliferation Assay

Cell proliferation of MCF-7 breast cancer cells was determined by [³H]thymidine incorporation (37, 38). Compounds were tested for their potential to either stimulate MCF-7 proliferation or inhibit proliferation. An EC_{50} or IC_{50} was determined for each compound tested. A compound's MCF-7 potency is defined as $pEC_{50} \times \%cpm_{max}$ (relative to estradiol) or $pIC_{50} \times \%cpm_{min}$ (relative to raloxifene) (cpm = radioactive counts per minute).

Ishikawa Endometrial Cell Stimulation Assay

The stimulation of human endometrial cells (Ishikawa cell line) was determined by increase in intrinsic alkaline phosphatase activity (39, 40). Compounds were tested for their potential to stimulate endometrial cells, as compared with estradiol. The $\%E_{max}$ is defined as 100 × (spectrophotometric reading at 405 nm with compound minus blank)/(spectrophotometric reading at 405 nm estradiol minus blank).

Data Reduction Methods

The multiplexed ERα LBD binding assay yielded relative fluorescence intensities for 405 compounds and 58 peptides. Figure 2B shows these intensities (*vertical axis*) plotted for each peptide tested (*horizontal axis*). The points representing the intensities for any given compound were connected with line segments to yield a *profile* (Spotfire DecisionSite, Spotfire, Inc., Somerville, MA). This 58-dimensional data set was simplified by applying PCA to yield the peptides (dimensions) deemed to provide most of the covariance in the data set. PCA was performed using the JMP application (SAS Institute, Cary, NC), yielding eigenvectors representing the relative contributions of the principal components to the total covariance. The 10 eigenvectors with greatest magnitude, representing approximately 99% of the covariance were selected. From these, peptides with coefficients greater than 0.25 were chosen for profile analysis. This resulted in a reduced data set, yielding profiles having 10 peptide dimensions (Fig. 2C).

These peptide binding profiles were subjected to hierarchical clustering according to profile *shape*. For each profile of N responses, all N(N-1)/2 pairwise differences were calculated and placed into a list. The distance between two such lists could then be characterized by their Euclidian distance. Using such a metric, agglomerative clustering was applied (unweighted pairwise group mean average, Fig. 3). Drawing a boundary through the clustering tree at a level yielding 12 clusters, and plotting profiles in a trellis arrangement by cluster ID gave a useful classification of profiles (Fig. 4). Cell assay data were similarly plotted as profiles. These data were limited in availability, and so were plotted without line segments connecting the data points. By arranging cell assay data profiles in a trellis using the 12 cluster IDs, the correspondence of peptide profile shape to cell assay results can be visually analyzed (Fig. 8).

Acknowledgments

We thank William Hoekstra, Steve Stimpson, Thomas Stanley, Dennis Heyer, and Timothy Willson for critical review of the manuscript and for many helpful discussions and sug-

REFERENCES

1. Shibata H, Spencer TE, Onate SA, Jenster G, Tsai SY, Tsai MJ, O'Malley BW 1997 Role of co-activators and co-repressors in the mechanism of steroid/thyroid receptor action. Recent Prog Horm Res 2:141–165
2. Hermanson O, Glass CK, Rosenfeld MG 2002 Nuclear receptor coregulators: multiple modes of modification. Trends Endocrinol Metab 13:55–60
3. Simoncini T, Hafezi-Moghadam A, Brazil DP, Ley K, Chin WW, Liao JK 2000 Interaction of oestrogen receptor with the regulatory subunit of phosphatidylinositol-3-OH kinase. Nature 407:538–541
4. Lee SR, Ramos SM, Ko A, Masiello D, Swanson KD, Lu ML, Balk SP 2002 AR and ER interaction with a p21-activated kinase (PAK6). Mol Endocrinol 16:85–99
5. Lazennec G, Thomas JA, Katzenellenbogen BS 2001 Involvement of cyclic AMP response element binding protein (CREB) and estrogen receptor phosphorylation in the synergistic activation of the estrogen receptor by estradiol and protein kinase activators. J Steroid Biochem Mol Biol 77:193–203
6. Bjornstrom L, Sjoberg M 2002 Signal transducers and activators of transcription as downstream targets of non-genomic estrogen receptor actions. Mol Endocrinol 16: 2202–2214
7. Kuiper GG, Enmark E, Pelto-Huikko M, Nilsson S, Gustafsson JA 1996 Cloning of a novel receptor expressed in rat prostate and ovary. Proc Natl Acad Sci USA 93:5925–5930
8. Moore JT, McKee DD, Slentz-Kesler K, Moore LB, Jones SA, Horne EL, Su JL, Kliewer SA, Lehmann JM, Willson TM 1998 Cloning and characterization of human estrogen receptor β isoforms. Biochem Biophys Res Commun 247:75–78
9. Harris HA, Katzenellenbogen JA, Katzenellenbogen BS 2002 Characterization of the biological roles of the estrogen receptors, ERα and ERβ, in estrogen target tissues *in vivo* through the use of an ERα-selective ligand. Endocrinology 143:4172–4177
10. Lindberg MK, Erlandsson M, Alatalo SL, Windahl S, Andersson G, Halleen JM, Carlsten H, Gustafsson JA, Ohlsson C 2001 Estrogen receptor α, but not estrogen receptor β, is involved in the regulation of the OPG/RANKL (osteoprotegerin/receptor activator of NF-κB ligand) ratio and serum interleukin-6 in male mice. J Endocrinol 171:425–433
11. McKenna NJ, O'Malley BW 2002 Minireview: nuclear receptor coactivators—an update. Endocrinology 143: 2461–2465
12. Shiau AK, Barstad D, Loria PM, Cheng L, Kushner PJ, Agard DA, Greene GL 1998 The structural basis of estrogen receptor/coactivator recognition and the antagonism of this interaction by tamoxifen. Cell 95:927–937
13. Pike AC, Brzozowski AM, Hubbard RE 2000 A structural biologist's view of the oestrogen receptor. J Steroid Biochem Mol Biol 74:261–268

EXHIBIT T

14. Pike AC, Brzozowski AM, Walton J, Hubbard RE, Thorsell AG, Li YL, Gustafsson JA, Carlquist M 2001 Structural insights into the mode of action of a pure antiestrogen. Structure 9:145–153

15. Heery DM, Kalkhoven E, Hoare S, Parker MG 1997 A signature motif in transcriptional co-activators mediates binding to nuclear receptors. Nature 387:733–736

16. Johnson BA, Wilson EM, Li Y, Moller DE, Smith RG, Zhou G 2000 Ligand-induced stabilization of PPARγ monitored by NMR spectroscopy: implications for nuclear receptor activation. J Mol Biol 298:187–194

17. Grese TA, Dodge JA 1998 Selective estrogen receptor modulators (SERMs). Curr Pharm Design 4:71–92

18. Faulds MH, Pettersson K, Gustafsson JA, Haldosen LA 2001 Cross-talk between ERs and signal transducer and activator of transcription 5 is E2 dependent and involves two functionally separate mechanisms. Mol Endocrinol 15:1929–1940

19. Simoncini T, Fornari L, Mannella P, Varone G, Caruso A, Liao JK, Genazzani AR 2002 Novel non-transcriptional mechanisms for estrogen receptor signaling in the cardiovascular system. Interaction of estrogen receptor α with phosphatidylinositol 3-OH kinase. Steroids 67:935–939

20. McKay LI, Cidlowski JA 1999 Molecular control of immune/inflammatory responses: interactions between nuclear factor-κ B and steroid receptor-signaling pathways. Endocr Rev 20:435–459

21. Valentine JE, Kalkhoven E, White R, Hoare S, Parker MG 2000 Mutations in the estrogen receptor ligand binding domain discriminate between hormone-dependent transactivation and transrepression. J Biol Chem 275:25322–25329

22. McKay LI, Cidlowski JA 1998 Cross-talk between nuclear factor-κ B and the steroid hormone receptors: mechanisms of mutual antagonism. Mol Endocrinol 12:45–56

23. Galien R, Garcia T 1997 Estrogen receptor impairs interleukin-6 expression by preventing protein binding on the NF-κB site. Nucleic Acids Res 25:2424–2429

24. Kousteni S, Chen JR, Bellido T, Han L, Ali AA, O'Brien CA, Plotkin L, Fu Q, Mancino AT, Wen Y, Vertino AM, Powers CC, Stewart SA, Ebert R, Parfitt AM, Weinstein RS, Jilka RL, Manolagas SC 2002 Reversal of bone loss in mice by nongenotropic signaling of sex steroids. Science [Erratum (299:1184)] 298:843–846

25. Iannone MA, Consler TG, Pearce KH, Stimmel JB, Parks DJ, Gray JG 2001 Multiplexed molecular interactions of nuclear receptors using fluorescent microspheres. Cytometry 44:326–337

26. Iannone MA 2001 Microsphere-based molecular cytometry. Clin Lab Med 21:731–742

27. Kellar KL, Iannone MA 2002 Multiplexed microsphere-based flow cytometric assays. Exp Hematol 30:1227–1237

28. Paige LA, Christensen DJ, Gron H, Norris JD, Gottlin EB, Padilla KM, Chang CY, Ballas LM, Hamilton PT, McDonnell DP, Fowlkes DM 1999 Estrogen receptor (ER) modulators each induce distinct conformational changes in ER α and ER β. Proc Natl Acad Sci USA 96:3999–4004

29. Norris JD, Paige LA, Christensen DJ, Chang CY, Huacani MR, Fan D, Hamilton PT, Fowlkes DM, McDonnell DP 1999 Peptide antagonists of the human estrogen receptor. Science 285:744–746

30. Northrop JP, Nguyen D, Piplani S, Olivan SE, Kwan ST, Go NF, Hart CP, Schatz PJ 2000 Selection of estrogen receptor β- and thyroid hormone receptor β-specific co-activator-mimetic peptides using recombinant peptide libraries. Mol Endocrinol 14:605–622

31. Scott JK, Smith GP 1990 Searching for peptide ligands with an epitope library. Science 249:386–390

32. Yu J, Smith GP 1996 Affinity maturation of phage-displayed peptide ligands. Methods Enzymol 267:3–27

33. Fairbrother WJ, Christinger HW, Cochran AG, Fuh G, Keenan CJ, Quan C, Shriver SK, Tom JY, Wells JA, Cunningham BC 1998 Novel peptides selected to bind vascular endothelial growth factor target the receptor-binding site. Biochemistry 37:17754–17764

34. Sidhu SS, Lowman HB, Cunningham BC, Wells JA 2000 Phage display for selection of novel binding peptides. Methods Enzymol 328:333–363

35. Willson TM, Norris JD, Wagner BL, Asplin I, Baer P, Brown HR, Jones SA, Henke B, Sauls H, Wolfe S, Morris DC, McDonnell DP 1997 Dissection of the molecular mechanism of action of GW5638, a novel estrogen receptor ligand, provides insights into the role of estrogen receptor in bone. Endocrinology 138:3901–3911

36. Edmunds JS, Fairey ER, Ramsdell JS 1997 A rapid and sensitive high throughput reporter gene assay for estrogenic effects of environmental contaminants. Neurotoxicology 18:525–532

37. Gottardis MM, Wagner RJ, Borden EC, Jordan VC 1989 Differential ability of antiestrogens to stimulate breast cancer cell (MCF-7) growth in vivo and in vitro. Cancer Res 49:4765–4769

38. Levenson AS, Jordan VC 1997 MCF-7: the first hormone-responsive breast cancer cell line. Cancer Res 57:3071–3078

39. Holinka CF, Hata H, Kuramoto H, Gurpide E 1986 Effects of steroid hormones and antisteroids on alkaline phosphatase activity in human endometrial cancer cells (Ishikawa line). Cancer Res 46:2771–2774

40. Littlefield BA, Gurpide E, Markiewicz L, McKinley B, Hochberg RB 1990 A simple and sensitive microtiter plate estrogen bioassay based on stimulation of alkaline phosphatase in Ishikawa cells: estrogenic action of δ 5 adrenal steroids. Endocrinology 127:2757–2762

41. Willson TM, Henke BR, Momtahen TM, Charifson PS, Batchelor KW, Lubahn DB, Moore LB, Oliver BB, Sauls HR, Triantafillou JA, Wolfe SG, Baer PG 1994 3-[4-(1,2-diphenylbut-1-enyl)phenyl]acrylic acid: a non-steroidal estrogen with functional selectivity for bone over uterus in rats. J Med Chem 37:1550–1552

42. McKenna NJ, Lanz RB, O'Malley BW 1999 Nuclear receptor coregulators: cellular and molecular biology. Endocr Rev 20:321–344

43. Huang HJ, Norris JD, McDonnell DP 2002 Identification of a negative regulatory surface within estrogen receptor α provides evidence in support of a role for corepressors in regulating cellular responses to agonists and antagonists. Mol Endocrinol 16:1778–1792

44. Shang Y, Brown M 2002 Molecular determinants for the tissue specificity of SERMs. Science 295:2465–2468

45. McDonnell DP, Clemm DL, Hermann T, Goldman ME, Pike JW 1995 Analysis of estrogen receptor function in vitro reveals three distinct classes of antiestrogens. Mol Endocrinol 9:659–669

46. Brzozowski AM, Pike AC, Dauter Z, Hubbard RE, Bonn T, Engstrom O, Ohman L, Greene GL, Gustafsson JA, Carlquist M 1997 Molecular basis of agonism and antagonism in the oestrogen receptor. Nature 389:753–758

47. Zajchowski DA, Kauser K, Zhu D, Webster L, Aberle S, White FA 3rd, Liu HL, Humm R, MacRobbie J, Ponte P, Hegele-Hartung C, Knauthe R, Fritzemeier KH, Vergona R, Rubanyi GM 2000 Identification of selective estrogen receptor modulators by their gene expression fingerprints. J Biol Chem 275:15885–15894

48. Levenson AS, Kliakhandler IL, Svoboda KM, Pease KM, Kaiser SA, Ward 3rd JE, Jordan VC 2002 Molecular classification of selective oestrogen receptor modulators on the basis of gene expression profiles of breast cancer cells expressing oestrogen receptor α. Br J Cancer 87:449–456

49. Lindberg MK, Moverare S, Eriksson AL, Skrtic S, Gao H, Dahlman-Wright K, Gustafsson JA, Ohlsson C 2002 Identification of estrogen-regulated genes of potential

EXHIBIT T

importance for the regulation of trabecular bone mineral density. J Bone Miner Res 17:2183–2195

50. Lannigan DA 2003 Estrogen receptor phosphorylation. Steroids 68:1–9

51. Zhu Y, Bond J, Thomas P 2003 Identification, classification, and partial characterization of genes in humans and other vertebrates homologous to a fish membrane progestin receptor. Proc Natl Acad Sci USA 100:2237–2242

52. Routledge EJ, White R, Parker MG, Sumpter JP 2000 Differential effects of xenoestrogens on coactivator recruitment by estrogen receptor (ER) α and ERβ. J Biol Chem 275:35986–35993

53. Bramlett KS, Wu Y, Burris TP 2001 Ligands specify coactivator nuclear receptor (NR) box affinity for estrogen receptor subtypes. Mol Endocrinol 15:909–922

54. Ding XF, Anderson CM, Ma H, Hong H, Uht RM, Kushner PJ, Stallcup MR 1998 Nuclear receptor-binding sites of coactivators glucocorticoid receptor interacting protein 1 (GRIP1) and steroid receptor coactivator 1 (SRC-1): multiple motifs with different binding specificities. Mol Endocrinol 12:302–313

55. Chang C, Norris JD, Gron H, Paige LA, Hamilton PT, Kenan DJ, Fowlkes D, McDonnell DP 1999 Dissection of the LXXLL nuclear receptor-coactivator interaction motif using combinatorial peptide libraries: discovery of peptide antagonists of estrogen receptors α and β. Mol Cell Biol 19:8226–8239

56. Heery DM, Hoare S, Hussain S, Parker MG, Sheppard H 2001 Core LXXLL motif sequences in CREB-binding protein, SRC1, and RIP140 define affinity and selectivity for steroid and retinoid receptors. J Biol Chem 276:6695–6702

57. McKenna NJ, O'Malley BW 2000 An issue of tissues: divining the split personalities of selective estrogen receptor modulators. Nat Med 6:960–962

58. Xu HE, Stanley TB, Montana VG, Lambert MH, Shearer BG, Cobb JE, McKee DD, Galardi CM, Plunket KD, Nolte RT, Parks DJ, Moore JT, Kliewer SA, Willson TM, Stimmel JB 2002 Structural basis for antagonist-mediated recruitment of nuclear co-repressors by PPARα. Nature 415:813–817

59. Connor CE, Norris JD, Broadwater G, Willson TM, Gottardis MM, Dewhirst MW, McDonnell DP 2001 Circumventing tamoxifen resistance in breast cancers using antiestrogens that induce unique conformational changes in the estrogen receptor. Cancer Res 61:2917–2922

60. Smith MM, Shi L, Navre M 1995 Rapid identification of highly active and selective substrates for stromelysin and matrilysin using bacteriophage peptide display libraries. J Biol Chem 270:6440–6449

61. Deng SJ, MacKenzie CR, Narang SA 1993 Simultaneous randomization of antibody CDRs by a synthetic ligase chain reaction strategy. Nucleic Acids Res 21:4418–4419

62. Deng SJ, MacKenzie CR, Narang SA 1995 Synthetic antibody gene libraries for in vitro affinity maturation. Methods Mol Biol 51:329–342

63. Pearce Jr KH, Potts BJ, Presta LG, Bald LN, Fendly BM, Wells JA 1997 Mutational analysis of thrombopoietin for identification of receptor and neutralizing antibody sites. J Biol Chem 272:20595–20602

64. Martinez E, Givel F, Wahli W 1987 The estrogen-responsive element as an inducible enhancer: DNA sequence requirements and conversion to a glucocorticoid-responsive element. EMBO J 6:3719–3727